

N72-32794

ACCRETION PROCESS OF THE MOON¹

Hitoshi Mizutani²

Seismological Laboratory, California Institute of Technology,
Pasadena, California 91109, USA

Takahumi Matsui and Hitoshi Takeuchi
Geophysical Institute, University of Tokyo,
Bunkyo-ku, Tokyo, Japan

¹Contribution No. 2104, Division of Geological and Planetary Sciences,
California Institute of Technology.

²On leave from Geophysical Institute, University of Tokyo.

ABSTRACT

Recent geochemical and geophysical data suggest that the initial temperature of the moon was strongly peaked toward the lunar surface. To explain such an initial temperature distribution, a simple model of accretion process of the moon is presented. The model assumes that the moon was formed from the accumulation of the solid particles or gases in the isolated, closed cloud. Two equations are derived to calculate the accretion rate and surface temperature of the accreting moon. Numerical calculations are made for a wide range of the parameters particle concentration and particle velocity in the cloud. A limited set of the parameters gives the initial temperature profiles as required by geochemical and geophysical data. These models of the proto-moon cloud indicate that the lunar outermost shell, about 400 km thick, was partially or completely molten just after the accretion of the moon and that the moon should have been formed in a period shorter than 1000 years. If the moon formed at a position nearer to the Earth than its present one, the moon might have been formed in a period of less than one year.

interior of the moon has been and/or is now cold (Kaula, 1969). More direct information on the interior temperature is obtained from analysis of the induction response of the moon to magnetic transients in the solar wind. According to the Sonett et al. (1971) analysis, the outer one thousand kilometers of the moon are now cool ($< 800^{\circ}\text{C}$), although the result depends on the assumed rock type and composition.

The first three constraints indicate a hot moon in the early stage of its evolution and the last one indicates a moon that is presently cool. The two inferences of the thermal state of the moon appear inconsistent with each other in view of conventional thermal history calculations and lead necessarily to the conclusion that the moon at a very early date was non-uniform, with chemical composition and temperature varying with radius, as discussed by Papanastassiou and Wasserburg (1971a). Ringwood (1966, 1971) suggests a notional lunar thermal history where the initial temperature increases from the center outwards, crossing the solidus in the outermost shell. Wood (1971) and Toksöz et al. (1971) also suggest that the initial temperature was highly peaked toward the lunar surface. In this paper, we will attempt to understand an initial temperature profile such that the deep interior is cool but the near-surface experiences at least partial melting in terms of an accretion model of the moon.

3: EARLY HEATING MECHANISMS

A few candidate mechanisms of early heating responsible for the non-uniform initial temperature have been proposed: (1) an accretional energy (Ringwood, 1971; Wood, 1971; Wood et al., 1971); (2) short-lived radioactive isotopes concentrated only in an outer shell (Wood, 1971);

and (3) electrical induction heating by an early intense solar wind (Sonett et al., 1968; Sonett et al., 1971).

As for the second mechanism, Schramm et al. (1970) have recently shown that there is no excess of ^{26}Mg , decay product of ^{26}Al , in meteorites. This observation limits significant ^{26}Al activity in the meteorites and possibly in the moon. In addition, we have no reason to suspect that short-lived radioactive elements would be preferentially located near the surface (Ringwood, 1971; Papanastassiou and Wasserburg, 1971a). Thus, the short-lived radioactivity as the early heating source must remain highly speculative.

The induction heating through a strong interplanetary electric field resulting from a premain sequence T-Tauri solar wind also heats not only the near-surface region but also the deep interior of the moon because the effect of the solar wind penetrates to the center of the moon due to the low conductivity throughout the early moon and low frequency of the variation of the solar wind. Therefore, the induction heating mechanism does not appear to be a probable process, contrary to the suggestions by Sonett et al. (1968, 1971).

On the other hand, an accretional heating is most promising because it is consistent with both the observation that the early highland formation and rapid cratering must have been simultaneous (e.g., Hartman, 1966) and the energy release as shown by Hanks and Anderson (1969). Therefore, we conclude that the accretional heating is a dominant early heating mechanism and that it resulted in an initial temperature distribution peaked near the surface. Since the accretional energy available for the lunar heating depends on the accretion process itself, the requirement of such a non-uniform initial temperature as described before

will give some information on the mode of the accretion of the moon.

4: MODEL OF ACCRETION PROCESS

Every theory of lunar origin assumes, explicitly or implicitly, that the moon was formed by the accretion of gas or small solid particles somewhere in the solar system. In the fission hypothesis, binary star hypothesis, and precipitation hypothesis, the moon is assumed to have been formed near the Earth. The capture hypothesis, on the other hand, assumes the moon was formed well beyond the gravity influence of the Earth. Any theory requires that coagulation of a cloud consisting of the solid particles or gas occurs to form the moon. For coagulation of the cloud to occur, the velocities of the particles in the cloud should be smaller than the escape velocity of the cloud and perturbations by other planets or by the sun should be much smaller than the gravity force of the proto-moon cloud. Otherwise the proto-moon cloud will be disrupted or dissipated for the moon is formed. Therefore, as a first approximation, we consider the proto-moon cloud to be an isolated system.

In a cloud consisting of solid particles of various sizes, inelastic collisions between particles take place and a large body grows at the expense of smaller bodies, because (1) the effective impact cross section of a large body is larger than that of a smaller body and (2) the fragmentation probability of a large body is smaller than that of a smaller body. Both effects suggest that the largest body in the proto-moon cloud will have become the nucleus of the moon.

We assume that the figure of the proto-moon cloud is a sphere or a slightly flattened ellipsoid. Schmidt (1957) proposed that the planets and satellites were formed from a ring-like cloud moving around the sun

or their parent planets; the proto-planets and proto-satellites grow by sweeping up the dust in the ring-like cloud (see also Safronov, 1959; Ruskol, 1960). It seems very difficult, however, to the present authors that the planets or satellites are formed from a ring-like cloud dispersed uniformly around their parents; deviatic velocities of the particles from Keplerian velocities in the cloud should cause the particle to converge on the parent star or to diverge from the system, not to encircle the embryo of the planets or the satellites. We note here that the accretion rate obtained by Safronov (1959) and Ruskol (1961) is, in essence, the rate for the case of the spherical cloud, not for the case of the ring-like cloud. It seems more probable that the proto-moon cloud takes the closed form, a sphere or a flattened ellipsoid, instead of the ring-like shape, although it may have developed from the ring-like swarm due to gravitational or rotational instability.

To summarize the features of the model described above and to define the model more explicitly, we list the assumptions on which the model studied below is based:

- (A1) The moon accreted from a proto-moon gas-dust cloud of roughly spherical shape in an isolated environment.
- (A2) The nucleus of the moon captures all of the impinging particles.
- (A3) The velocity distribution of the particles far from the nucleus is expressed by a Maxwell-Boltzmann distribution. The particle velocity referred to here is the velocity relative to the nucleus; the cloud itself may move as a whole around the sun of the Earth.
- (A4) The velocity distribution of the particles far from the nucleus does not change with time, except through the concentration of the particles which decreases with the growth of the moon.

(A5) The shrinkage of the cloud as a whole is not taken into account; the gravity force of the cloud is assumed to be dynamically balanced with the kinetic energy of the particle.

(A6) Total mass of the proto-moon cloud is equal to the present moon's mass.

(A7) Spin angular momentum of the proto-moon is too small to affect the accretion rate.

5: FUNDAMENTAL EQUATIONS

As assumed in (A3), let the velocity distribution of the particles far from the nucleus be expressed by:

$$f(v) = \frac{4\pi N(t) v^2}{(c\sqrt{\pi})^3} \exp\left(-\frac{v^2}{c^2}\right) \quad (1)$$

where v is the velocity (relative to the nucleus) of the particles far from the nucleus, c is the most probable speed which is $0.924 \times$ mean velocity, and $N(t)$ is the concentration (by mass) of the particles in the cloud. The equation represents an isotropic Maxwell-Boltzmann velocity distribution. The particles moving in random directions sometimes enter into the region of the gravity influence of the embryo of the moon and are captured by it. In this case accretion rate of the proto-moon can be written as follows (see Singer and Bandermann, 1970, for derivation):

$$\frac{dM(t)}{dt} = 2\sqrt{\pi} R(t)^2 N(t) c \left\{ 1 + \frac{2GM(t)}{c^2 R(t)} \right\} \quad (2)$$

where $M(t)$ and $R(t)$ are mass and radius of the growing moon, respectively, and G is the universal gravitational constant. The second term in the bracket in (2) represents the apparent increase of the cross section of the nucleus due to the gravitational capture.

From (A5), the time variation of the particle concentration $N(t)$ is given by

$$N(t) = \frac{1}{V_0} (M - M_0(t)) = \frac{N_0}{M_0} (M_0 - M(t)) \quad (3)$$

where M_0 and V_0 are the total mass and the volume of the proto-moon cloud, and N_0 is the initial particle concentration (by mass) in the cloud.

Thus, if we are given c (most probable speed of the particle) and N_0 (initial particle concentration) or V_0 (initial volume of the cloud), we can calculate the accretion rate and hence the radius of the moon as a function of time through (2).

When

$$c \ll \sqrt{2GM(t)/R(t)} \quad (4)$$

eq. (2) is reduced to a simple form:

$$\frac{dR}{dt} = A \left\{ R_0^3 - R(t)^3 \right\} R^2(t) \quad (5)$$

where

$$A = \frac{4}{3} \sqrt{\pi} \frac{N_0 G}{R_0^3 c} \quad (6)$$

and R_0 = the present radius of the moon.

From (5) we see that the accretion rate starts from zero, accelerates as the moon grows, and finally goes to zero as the moon's radius approaches its present one, although $dR/dt = 0$ at $R = 0$ is not real because (4) is violated at $R = 0$. In addition, it should be noted that all the unknown parameters are absorbed in the factor A which determines the time scale of the accretion process; the accretion rate reaches to a maximum at $R(t) = (2/5)^{1/2} R_0 = 0.737 R_0$ irrespective of N_0 and c . As is known from eq. (4), the moon approaches the present radius exponentially in the final stage and it takes infinite time for the moon to reach the exact present size, although the major part of the moon is, of course, built up in a finite time.

The thermal effect of the accretion process can be obtained from the consideration of the energy balance on the lunar surface (e.g., Benfield, 1950). Energies imparted to the proto-moon are the kinetic and potential energies of the incoming material. The energy will be absorbed in the following ways: (1) in raising the temperature of the incoming material, including possible phase changes, (2) as radiation energy back into outer space, (3) in warming the interior of the moon by conduction or convection from the surface. Therefore we have the following equation to represent the energy balance per unit area on the surface:

$$\rho \left(\frac{c^2}{2} + \frac{GM(t)}{R(t)} \right) \frac{dR(t)}{dt} = \quad (7)$$

$$\varepsilon \sigma \left\{ T^4(R, t) - T_a^4 \right\}$$

$$+ \left\{ \rho C_p (T(R, t) - T_f) + \rho L \right\} \frac{dR(t)}{dt}$$

$$+ k \left(\frac{\partial T}{\partial r} \right)_{r=R}$$

where the following notations are used:

- P: the density of the incoming material,
- ϵ : emissivity of the moon's surface,
- σ : Stefan-Boltzmann constant
- T_a : the radiative equilibrium temperature of the proto-moon cloud,
- T_b : the temperature of the incoming material as it enters the proto-moon's gravitational field,
- L: the heat of fusion of the incoming material per unit weight,
- K: the thermal conductivity at the lunar surface.

The last term in (7) may certainly be neglected because the magnitude of the term is orders of magnitude smaller than the other terms. The term of heat of fusion is taken into account when the temperature exceeds the solidus. The effect of adiabatic compression is neglected here because the rise in temperature due to adiabatic compression amounts to only $30 \sim 50^\circ\text{C}$ even at the center of the moon. Thus (7) can be used to determine the surface temperature of a moon growing with accretion rate dR/dt given by (2). The initial temperature profile in the moon after full accretion is obtained by tracing the surface temperature of the accreting moon as a function of radius, because the effect of the thermal conduction and radioactive heat source during accretion is negligibly small.

Physical parameters used in the calculations present here are listed in Table I.

6: RESULTS

We have calculated the accretion rate and initial temperature distribution for a wide range of the assumed initial particle concentration

of the cloud ($10^{-8} \leq N_0 \leq 10^{-3} \text{ g/cm}^3$) and the assumed most probable speed of the particle ($3 \times 10^1 \leq c \leq 3 \times 10^5 \text{ cm/sec}$).

In Fig. 7 are shown the variations of the accretion rate dR/dt with radius for the case of $N_0 = 10^{-8} \text{ g/cm}^3$ and $c = 3000, 300, 30$ and 3 m/sec . As has been indicated in (5) and (6), the accretion rate is inversely proportional to c when the gravity force of the moon becomes strong enough to capture the particles by its own gravity. Except in the case of $c = 3 \text{ km/sec}$, which is larger than the escape velocity of the present moon, every curve of the accretion rate in Fig. 1 has a maximum at $r \sim 1300 \text{ km}$, above which the accretion rate decreases rapidly. This feature of the accretion rate has a pronounced effect on the initial temperature profile of the moon.

Fig. 2 is a typical example of the radial growth of the moon as a function of time. Although it takes infinite time for the moon to reach the exact present size, the major part of it is formed in a relatively short time. It is to be noted that it takes almost the same period for the proto-moon to reach asteroid size (a few hundred kilometers) from 10 kilometers in radius as that required for the moon to grow to $r \approx 1700 \text{ km}$ from asteroid size. The accretion time, t_{acc} , is defined here as the period during which the proto-moon grows from $r = 100 \text{ km}$ to $r = 1700 \text{ km}$, 98% of the present moon's radius. In the case shown in Fig. 2, the accretion time is about 60 years.

Initial temperature profiles calculated for choices of N_0 and c are shown in Figs. 3 and 4. Fig. 3 illustrates the dependence of the initial temperature profile on the assumed most probable particle velocity. When the size of the proto-moon is small, the temperature is affected mainly by the kinetic energy of the incoming material; the higher particle

velocity gives the higher temperature at this stage. After the proto-moon grows to the size larger than a few hundred kilometers, the gravitational capture becomes significant and the lower particle velocity begins to give the higher temperature.

The curve corresponding to $c = 3\text{m/sec}$ and $N_0 = 10^{-8} \text{ g/cm}^3$ is very similar to the initial temperature proposed by Ringwood (1971) and is consistent with non-uniform initial temperature models of Wood (1971) and Papanastassiou and Wasserburg (1971a) as well. The temperature profile indicates that the outermost shell about 400 km thick is partially or completely molten. The extensive melting of the near-surface region may provide the early differentiation including the highland formation in such a way as described by Wood et al. (1971). The high temperature during the final accretion stage is also consistent with the strong depletion of volatile elements and enrichment of refractory elements. On the other hand, the initial temperature profiles corresponding to the particle velocities larger than 30 m/sec are too low to cause the differentiation just after the accretion of the moon.

Fig. 4 illustrates the dependence of the initial temperature on the original particle concentration N_0 in the cloud; the model with the higher particle concentration gives the higher initial temperature. The initial temperature corresponding to the model of particle concentration N_0 larger than 10^{-7} g/cm^3 is high enough in the near-surface region to cause the early extensive differentiation and is low enough in the central part to suggest the present low temperature throughout the moon. Therefore, among the parameters in Fig. 4, the parameters of $N_0 \geq 10^{-6} \text{ g/cm}^3$ and $c = 300 \text{ m/sec}$ give a reasonable initial temperature distribution in view of the aforementioned constraints on the thermal evolution of the moon.

We can limit the assumed parameters N_0 and C by examining the initial temperature profiles obtained for the parameters. Fig. 5 is a diagnostic diagram for this purpose and a summary of the numerical results calculated in this paper. The diagram is divided into four regions on the basis of the initial temperature distributions obtained. In "A" region, every initial temperature at $r = 0 \sim 1000$ km exceeds 1000°C and it is considered to be too high to explain the present low temperature of the moon. The initial temperatures with parameters in "D" region do not exceed the solidus at the outermost shell and they are inconsistent with early extensive differentiation. The initial temperature profiles in region "B" and "C" are appropriate for our view of lunar thermal evolution; the temperature in the central part is low enough, and the temperature near the lunar-surface exceeds the solidus or liquidus. The boundary between B and C regions is drawn, for the sake of convenience, to indicate that the peak-temperatures of the initial temperature profiles in B region exceed $T = 2500^\circ\text{K}$ which may be too high to explain the apparent quiescence of the lunar igneous activity during the first 0.5 billion years after the formation of the moon (Papanastassiou and Wasserburg, 1971b; Compston et al., 1971). This reasoning to reject the parameters in B region should, however, wait for the detailed analysis of the subsequent thermal history of the moon and further datings of the lunar rocks. In Fig. 5 are shown the iso-accretion time contours. The accretion times for the parameters in region C and D are less than 1000 years; accretion time of the moon should be less than 1000 years to yield the initial temperature consistent with several geophysical and geochemical data.

7: DISCUSSION

So far we have assumed that the most probable speed of the particle is independent of the particle concentration in the cloud. But if the cloud is in a statistically steady state, the particle speed should be related with particle concentration in the cloud, because the dynamics of the isolated cloud consisting of the solid particles is equivalent to the n-body problem of classical dynamics, in which we have a well known virial theorem relating the kinetic energy with potential energy of the system. When the particles in the cloud are all of the same mass, the most probable speed of the particles, C in eq. (1), is obtained easily from the virial theorem (Chandrasekhar, 1943, p. 200):

$$C = \left(\frac{GM}{3R} \right)^{\frac{1}{2}} = \left(\frac{4\pi}{81} G^3 M^2 N_0 \right)^{\frac{1}{6}} \quad (8)$$

where M and R are the total mass and radius of the cloud, respectively. The above equation means that the most probable speed of the particles is $1/6$ times the escape velocity of the cloud. In Fig. 5 is also shown the relation between C and N_0 obtained from (8). In deriving (8), it was assumed that the particles in the cloud have the same mass and that the system is non-dissipative in energy.

The effects of the size distribution and inelastic collisions on the velocity distribution are difficult to estimate but probably both will lower the value of c given by (8). Therefore, (8) should be considered a rough estimate of the most probable particle speed C , or to indicate the upper limit of C for a given N_0 . Nevertheless (8) is still important because we can considerably limit the range of possible C and N_0 in Fig. 5.

One more constraint for the range of possible C and N_0 comes from the consideration of stability against tidal disturbance. As assumed in (A1), the proto-moon is stable with respect to the tidal disturbances by the sun or the Earth. The condition of the stability is represented by Roche density: the density in the cloud should be larger than the Roche density specified for a particular disturbing body and the distance from it. Although we have different definitions of Roche density for different assumptions on the primary body and the secondary body, the order of its magnitude is

$$\rho^* \approx M / R^3 \quad (9)$$

where M is the mass of the primary (perturbing) body, and R is the distance between the perturbed body and the perturbing body (Jeans, 1929). The Roche density for the sun gives ρ_{\odot}^* equal to $6 \times 10^{-7} \text{ g/cm}^3$ at the distance of 1 A.U. from the sun, and the Roche densities for the Earth give $\rho_{\oplus}^* = 10^{-4} \text{ g/cm}^3$ and $\rho_{\oplus}^* = 1.3 \times 10^{-3} \text{ g/cm}^3$ at the distances of 60 Earth radii and 30 Earth radii from the Earth, respectively. Therefore, as shown in Fig. 5, if the moon is formed from a sun-orbiting swarm at 1 A.U., the major part of the moon should have been formed in a period shorter than 100 years. And if the moon is formed from a proto-moon cloud situated at the position nearer than the present position from the Earth, the moon should have been formed in a period shorter than 1 year. Such a short time scale for the formation as those found here seems surprising compared with the geological time scale but it is nevertheless necessary to obtain the appropriate initial temperature distribution. It is also to be noted that the estimate of the accretion time in Fig. 5 does not depend significantly on the details of the model because the accretion rate is primarily determined by the required initial temperature

distribution. But the way to connect the accretion rate with the physical parameters of the proto-moon cloud depends on the model itself. All the assumptions made in this paper, except (A5), tend to give a higher accretion rate for given parameters N_0 and C . Therefore the accretion times mentioned above for the sun-bound cloud and for the Earth-bound cloud may be minimum and they may be increased up to 1000 years but not much more.

Thermal history calculations using the initial temperature distributions calculated in the present paper show that the lunar interior deeper than 400 km from the surface has never been melted (Mizutani et al., 1971; see also Toksöz et al., 1971). This indicates that the deep interior of the moon may be composed of the primordial matter, as suggested from the interpretation of the electrical conductivity profile of the moon by Sonett et al. (1971).

8: EFFECT OF ANGULAR MOMENTUM

The accretion rate may be affected by the existence of axial rotation of the proto-moon cloud as has been pointed out by Phinney (1971), and we will briefly consider the effect of the axial rotation on the accretion rate. Assume the spin angular momentum of the proto-moon cloud to be the same as that of the present moon, and also assume rigid rotation of the proto-moon cloud. Then the rotational velocity is maximum at the equatorial periphery of the proto-moon cloud and is written from the conservation law of the angular momentum as follows:

$$\frac{V_{\text{cloud}}}{V_{\text{present}}} = \frac{R_{\text{present}}}{R_{\text{cloud}}}$$

where V_{cloud} and R_{cloud} are rotational velocity and radius of the proto-

moon cloud, respectively, and v_{present} and R_{present} are the same quantities for the moon in its present state. v_{present} (at the lunar surface) is about 4 m/sec, while $R_{\text{cloud}}/R_{\text{present}}$ is probably larger than 10 which corresponds to a particle concentration of the cloud of about 3×10^{-3} g/cm³. Thus the rotational velocity in the proto-moon cloud is less than 0.4 m/sec. This value is very small compared with the presumed random particle velocity estimated from the virial theorem. Therefore the motion of the particles in the cloud could not be affected significantly by the axial rotation of the proto-moon cloud, although a fraction of the particles, of course, may enter orbital motion around the proto-moon nucleus and remain uncaptured by the nucleus. The effect of the axial rotation of the cloud will possibly become significant in the final stage of the accretion process, after all particles in non-circumferential orbits are captured by the moon. When the remaining particles are all in the circumferential orbit around the proto-moon, the accretion rate cannot be expressed by (4), which is based on the assumption that the velocities of the particles are statistically isotropic and random. The orbiting particles remain uncaptured and may grow independently of the moon until the perturbations by the sun or the Earth deflect them from their orbit. Such particles may have grown up to a few hundred kilometers by that time and may bombard the lunar surface up to about one billion years after the formation of the moon. This may give a mechanism of a late major bombardment which may have triggered melting of the near-surface layer and formed circular maria (Papanastassiou and Wasserburg, 1971b).

9: CONCLUSION

Assuming the moon was formed by the accumulation of small solid or

gaseous particles in an isolated and closed cloud, we have shown that the non-uniform initial temperature required by geochemical and geophysical data is realizable under appropriate conditions of the proto-moon cloud. The probable initial temperature distribution calculated here indicates that the outermost region of the moon ($1300 \leq r \leq 1700$ km) was partially or completely molten just after the full accretion of the moon. To yield such an initial temperature the major part of the moon should have been formed in a period shorter than 1000 years; the above estimate of the accretion time does not depend on the details of the model. If the moon is formed at a position significantly closer to its present position from the Earth, the moon may have been formed in a period shorter than 1 year. Necessary physical conditions of the proto-moon cloud are that the concentration of the particle in the cloud is larger than 10^{-7} g/cm³ and that the most probable relative speed of the particles is less than $\sim 10^4$ cm/sec. This condition does not exclude any theory of lunar origin, but high particle concentrations in the cloud and low relative particle velocities favor a moon accreting near the Earth.

Although the short time scale of the accretion process seems inconsistent with the prolonged meteorite impacts which probably created circular mare basins, the introduction of angular momentum to this model may resolve the problem; a minor fraction of the particles in the proto-moon cloud are trapped in Keplerian orbits around the moon, grow independently of the moon to a few hundred kilometers in size, and finally are captured by the moon due to the Earth's or Sun's perturbations, as late as 1.0 billion years after the formation of the moon.

ACKNOWLEDGMENTS

We wish to thank T. C. Hanks who kindly read through the manuscript and gave valuable suggestions towards improving the manuscript. We acknowledge D. L. Anderson and L. Thomsen for their interest and encouragement. We are also grateful to A. E. Ringwood and N. Fujii for their helpful comments on the early version of this paper.

This research was partially supported by National Aeronautics and Space Administration contract NASA NGL 05-002-069.

REFERENCES

- Benfield, A. E., The temperature in an accreting earth, Trans. Amer. Geophys. Union, 31, 53, 1950.
- Chandrasekhar, S., Principles of Stellar Dynamics, Dover Publication, Inc., New York, 1943, Chapter V, p. 193.
- Compston, W., M. J. Vernon, H. Berry, and R. Rudowski, The age of the Fra Mauro formation: A radiometric older limit, Earth Planet. Sci. Letters, 12, 55, 1971.
- Ganapathy, R., R. R. Keays, J. C. Land, and E. Anders, Trace elements in Apollo 11 lunar rocks: Implications for meteorite influx and origin of the moon, Geochim. Cosmochim. Acta, Suppl., 1, 34, 1117, 1970.
- Hanks, T. C., and D. L. Anderson, The early thermal history of the earth, Phys. Earth Planet. Interiors, 2, 19, 1969.
- Hartmann, W. K., Early lunar cratering, Icarus, 5, 406, 1966.
- Hinners, N. W., The new moon: A review, Rev. Geophys. Space Phys., 9, 447, 1971.
- J Jeans, J. H., Astronomy and Cosmogony, 2nd ed., Cambridge University Press, 1929, p. 232 and p. 263.
- Kaula, W. M., Interpretation of lunar mass concentrations, Phys. Earth Planet. Interiors, 2, 123, 1969.
- Mizutani, H., T. Matui, and H. Takeuchi, Thermal history of the moon, in preparation, 1971.
- Papanastassiou, D. A., and G. J. Wasserburg, Lunar chronology and evolution from Rb-Sr studies of Apollo 11 and 12 samples, Earth Planet. Sci. Letters, 11, 37, 1971a.
- Papanastassiou, D. A., and G. J. Wasserburg, Rb-Sr ages of igneous rocks from the Apollo 14 mission and the age of the Fra Mauro formation, Earth Planet. Sci. Letters, 12, 36, 1971b.

- Phinney, R. A., A comment on this paper at "Lunar Geophysics" Conference held at Lunar Science Institute, Houston, October 18-21, 1971.
- Ringwood, A. E., Chemical evolution of the terrestrial planets, Geochim. Cosmochim. Acta, 30, 41, 1966.
- Ringwood, A. E., Petrogenesis of Apollo 11 basalts and implications for lunar origin, J. Geophys. Res., 75, 6453, 1971.
- Ringwood, A. E., and E. Essene, Petrogenesis of Apollo 11 basalts, internal constitution and origin of the moon, Geochim. Cosmochim. Acta, Suppl. 1, 34, 769, 1970.
- Ruskol, E. L., The origin of the moon, I. Formulation of a swarm of bodies around the earth, Sov. Astron. AJ, 4, 657, 1960.
- Safronov, V. S., On the primeval temperature of the earth, Bull. Acad. Sci. USSR, Geophys. Ser. (English Transl.), 1, 85, 1959.
- Schmidt, O. J., A Theory of the Origin of the Earth: Four Lectures, Lawrence & Wishart, London, 1959.
- Schramm, D. N., F. Tera, and G. J. Wasserburg, The isotopic abundance of ^{26}Mg and limits on ^{26}Al in the early solar system, Earth Planet. Sci. Letters, 10, 44, 1970.
- Singer, S. F., and L. W. Bandermann, Where was the moon formed?, Science, 170, 438, 1970.
- Sonett, C. P., D. S. Colburn, and K. Schwartz, Electrical heating of meteorite parent bodies and planets by dynamo induction from a pre-main sequence T Tauri "Solar Wind," Nature, 219, 924, 1968.
- Sonett, C. P., D. S. Colburn, P. Dyal, C. W. Parkin, B. F. Smith, G. Schubert, and K. Schwartz, Lunar electrical conductivity profile, Nature, 230, 359, 1971.

Toksdz, M. N., S. Solomon, J. Minear, and D. Johnson, Abstract of "Lunar Geophysics" Conference held at Lunar Science Institute, Houston, October 18-21, 1971.

Urey, H. C., and G. J. F. MacDonald, Origin and history of the moon, in Physics and Astronomy of the Moon, 2nd ed., edited by Z. Kopal, Academic Press, New York, 1971, Chapter 6, p. 213-289.

Wood, J. A., Petrology of the lunar soil and geophysical implications, J. Geophys. Res., 75, 6497, 1971.

Wood, J. A., U. B. Marvin, J. B. Reid, Jr., G. J. Taylor, J. F. Bower, B. N. Powell, and J. S. Dickey, Jr., Mineralogy and petrology of the Apollo 12 lunar sample, Smithsonian Astrophysical Observatory, Special Report 333, 1971.

Table 1. Parameters used in the present calculation.

M_0	: Present lunar mass = 7.343×10^{25} g
R_0	: Present lunar radius = 1739 km
r_0	: Initial radius of the nucleus of the moon = 10 km
ρ	: Density of the accreting material = 3.34 g/cm^3
T_a	: Radiative equilibrium temperature of the proto-moon cloud = 300°k
T_b	: Original temperature of the accreting material = 300°k
L	: Heat of fusion = 4.18×10^9 erg/g
C_p	: Specific heat = 1.30×10^7 erg/g
T_s	: Solidus temperature in the moon $T_s(r)^* = 2000 - 2.08 \times 10^{-4} r^2$ (km), $^\circ\text{k}$
T_L	: Liquidus temperature = $T_s(r) + 100^\circ\text{k}$
ϵ	: Emissivity = 1.0
σ	: Stefan-Boltzmann constant = $5.67 \times 10^{-5} \text{ erg/cm}^2 \cdot \text{g} \cdot \text{K}^4$
G	: Universal gravitational constant = $6.67 \times 10^{-8} \text{ dyn/cm}^2 \cdot \text{g}^2$

*Based on the data by Ringwood and Essene (1970).

FIGURE CAPTIONS

Fig. 1: Variation of accretion rate with radius.

Fig. 2: Radial growth of the moon with time for the case of $N_0 = 10^{-6} \text{ g/cm}^3$ and $C = 100 \text{ m/sec}$.

Fig. 3: Initial temperature profiles for the cases of $N_0 = 10^{-8} \text{ g/cm}^3$ and $C = 3 \sim 3000 \text{ m/sec}$. Note the dependence of the initial temperature profile on the particle velocity C .

Fig. 4: Initial temperature profiles for the cases of $C = 300 \text{ m/sec}$ and $N_0 = 10^{-4} \sim 10^{-8} \text{ g/cm}^3$. The numerals attached to the curves show N_0 used.

Fig. 5: A summary of the calculations. Thick curves are boundaries of A, B, C, and D regions, each of which represents a characteristic feature of the initial temperature (see text). Thin dotted curves are iso-accretion time contours. The numbers attached on the curves indicate the period during which the moon grows from $r = 10 \text{ km}$ to $r = 1700 \text{ km}$. The shaded zone indicates a $C-N_0$ region conceivable from the virial theorem. The lower boundary of the region is uncertain. The Roche densities for the sun and the earth are indicated just above the abscissa.

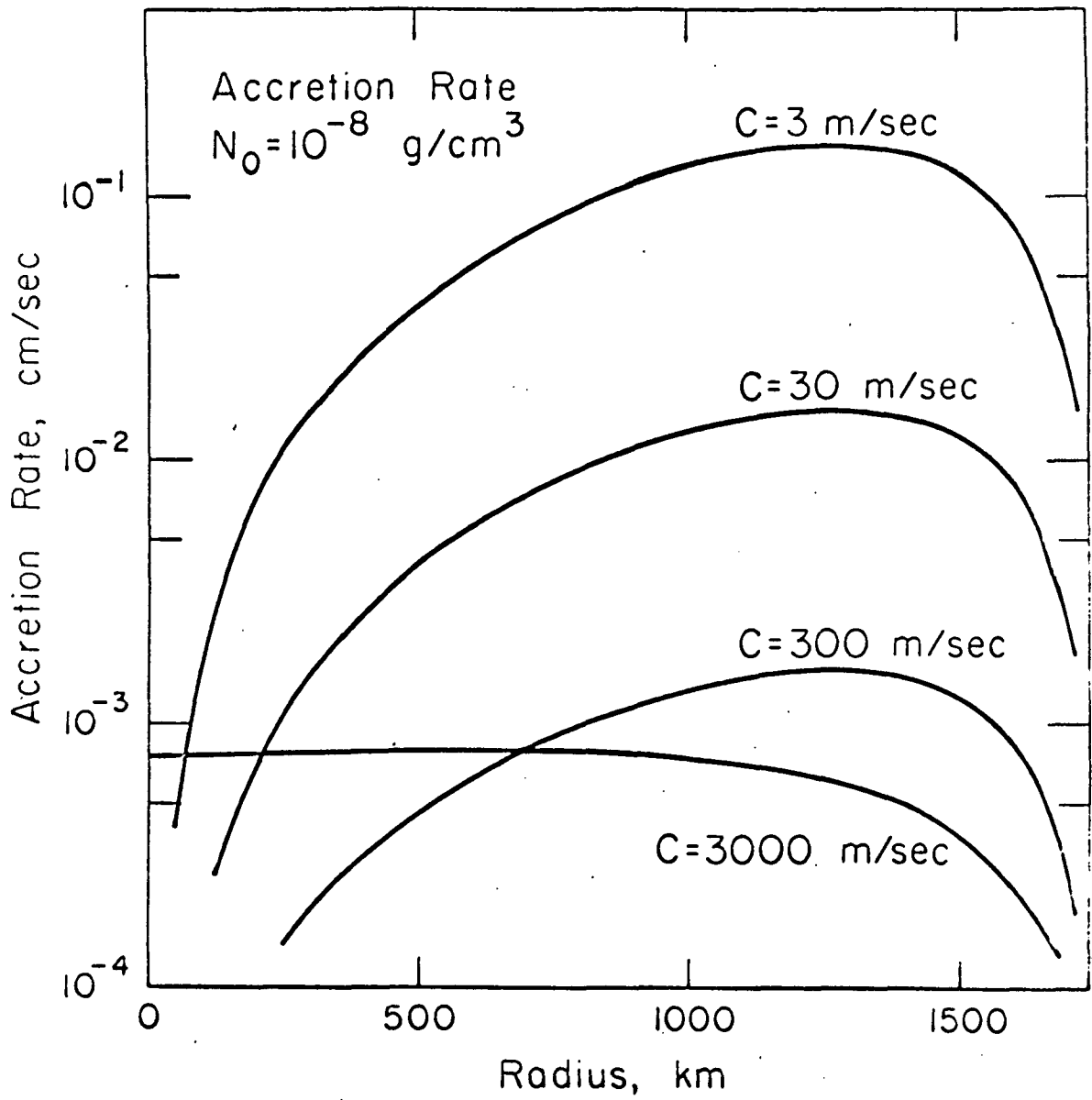
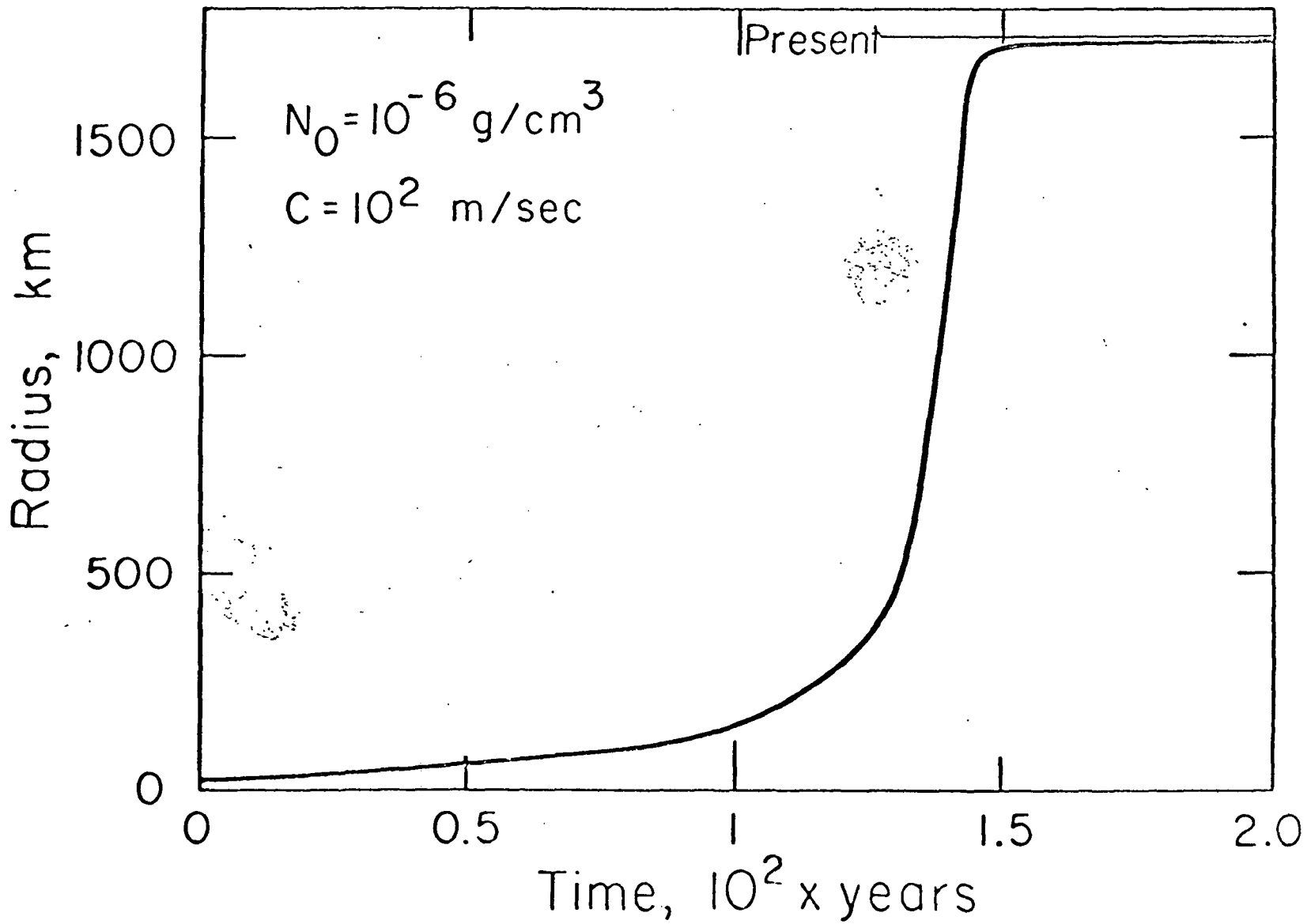


Figure 1



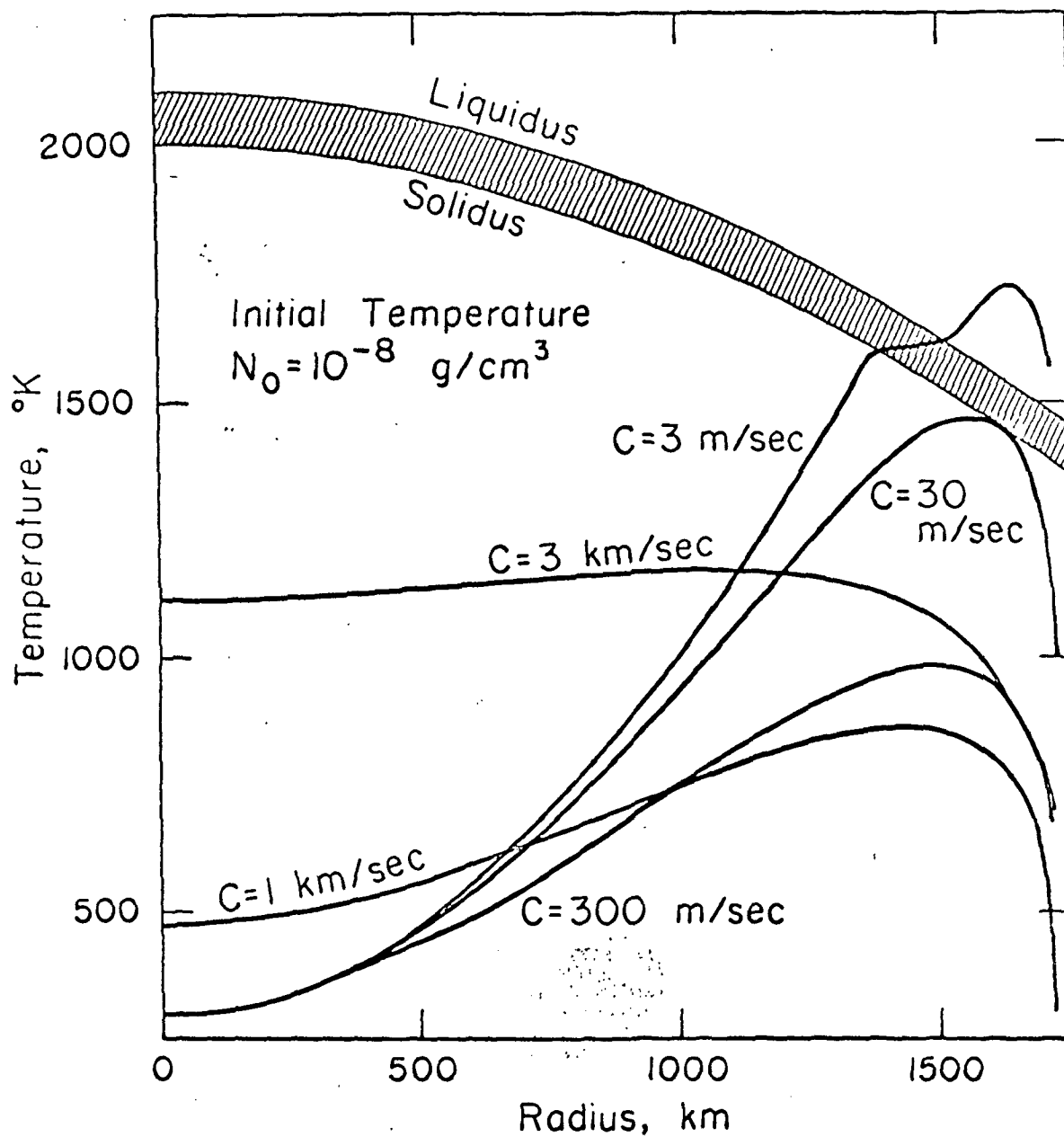


Figure 3

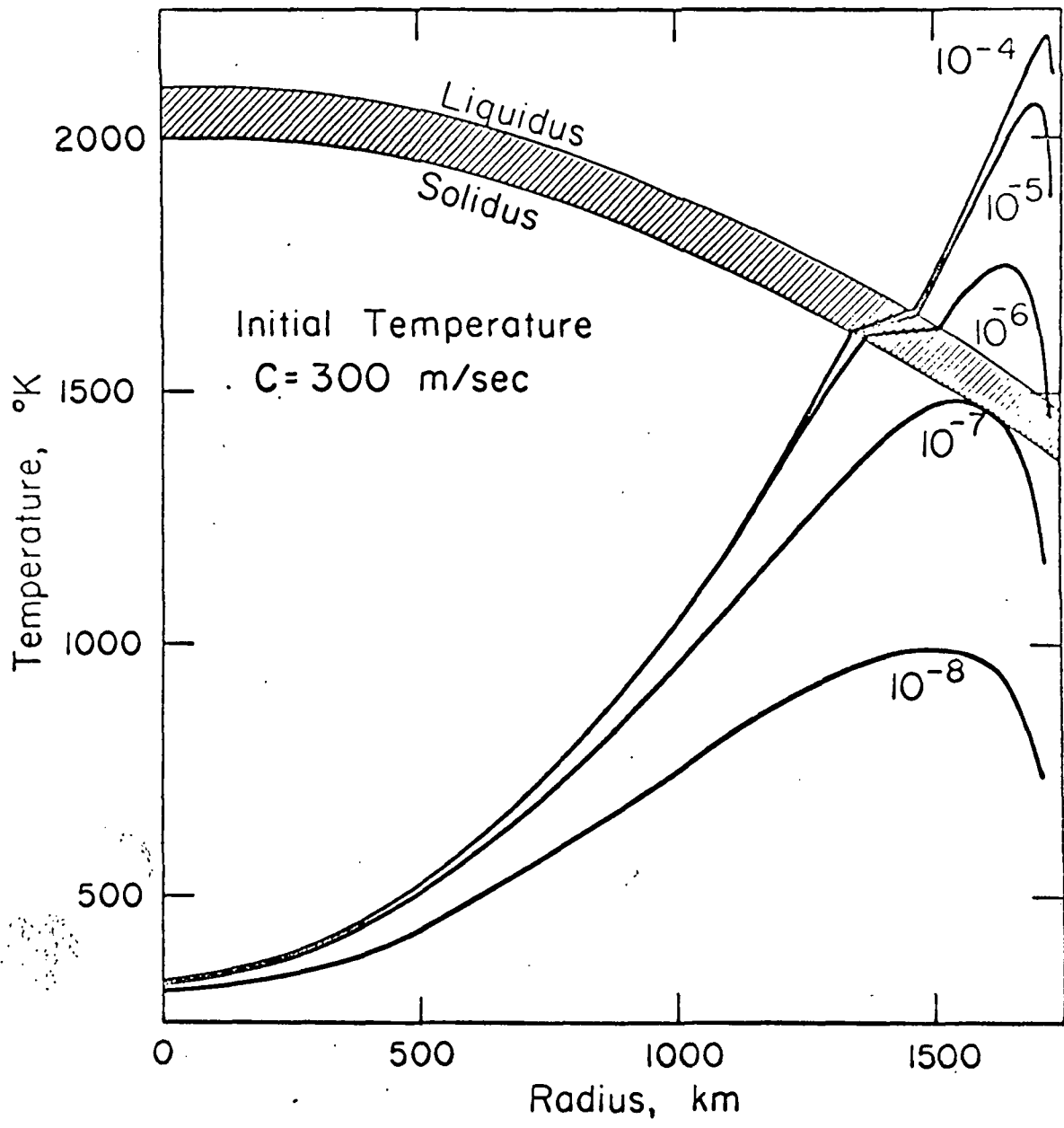


Figure 4

Fig. 5

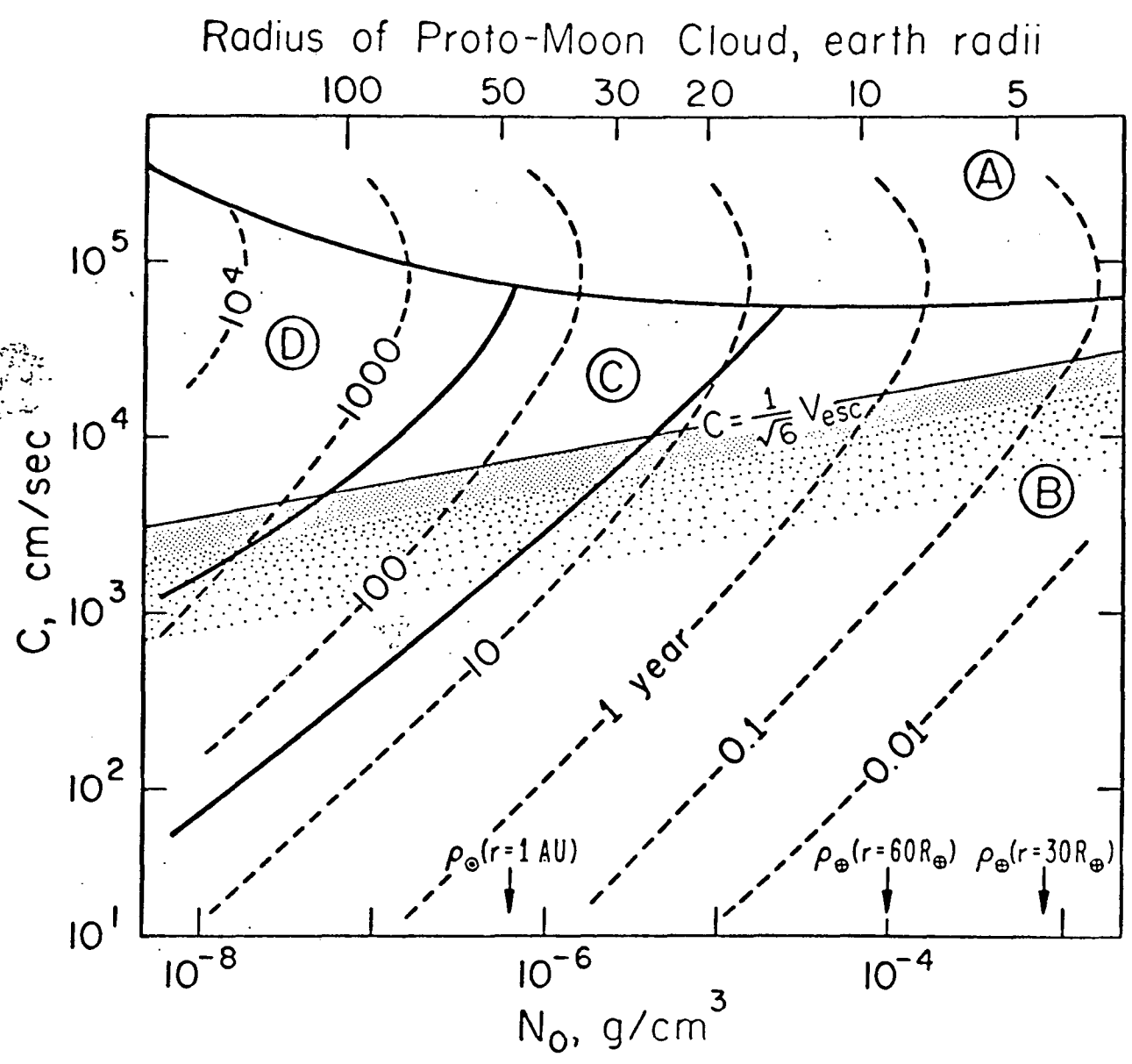


Figure 5